Higher-Order Homogenization of Initial/ Boundary-Value Problem

Jacob Fish and Wen Chen

Departments of Civil, Mechanical and Aerospace Engineering

Rensselaer Polytechnic Institute, Troy, NY 12180, USA

Abstract: Higher-order homogenization of initial/boundary-value problem with oscillatory coefficients in one-dimension is studied. Validity range and limitations of the theory are established. We show that the higher terms are necessary to account for wave dispersion, but introduce secular terms which grow unbounded in time. Numerical procedures requiring superconvergent recovery of higher order derivatives are described.

Keywords: homogenization, higher-order, dispersion, dynamics, composite materials, multiple scales

1. Introduction

The internal material interfaces in composite materials cause reflection and refraction of stress waves, giving rise to dispersion and attenuation of waves within material microstructure [1]. In an early study, Moon [3] proposed a continuum model based on the effective modulus concept. This formulation leads to a theory that is non-dispersive and therefore somewhat limited. Simulation of response phenomena associated with the material microstructure, such as wave dispersion, requires a higher-order continuum description [4]. The effective stiffness theory developed by Sun, Achenbach and Herrmann [5][6] is the first of the dispersive continuum models for composites. Subsequently, several higher-order homogenization based theories have been proposed (see Bedford and Stern [7][8], Hegemier, Gurtman and Nayfeh [9][10], and Boutin and Auriault [17]). For an excellent survey of various higher order continuum models in elastodynamics of composites, we refer to [11].

The use of multiple-scale expansions as a systematic tool of averaging for problems other than elastodynamics can be traced to Sanchez-Palencia [14], Benssousan, Lions and Papanicoulau [12], Bakhvalov and Panasenko [13]. The role of higher order terms has been investigated in statics by Gambin and Kroner [15], and Boutin [16]. In elastodynamics, Boutin and Auriault [17] demonstrated that the terms of a higher order successively introduce effects of polarization, dispersion and attenuation.

So far various approaches utilizing higher order homogenization theory in elastodynamics were limited to a single-frequency wave dependence. In this work we focus on a general initial/boundary-value problem in a periodic heterogeneous medium. Attention is restricted to one-dimensional initial/boundary-value problems in an attempt to construct a closed-form analytical solution for a model problem. Validity range and limitations of the

theory in elastodynamics are established. We show that the higher order theory is necessary to account for wave dispersion, but introduces secular terms which grow unbounded in time. Numerical procedures requiring superconvergent recovery of higher order derivatives are also described.

The outline of this paper is as follows. Problem statement and high-order homogenization are formulated in Section 2. Analytical solutions and numerical procedures are presented in Section 3. Section 4 gives numerical examples. We conclude with some remarks and discuss future work in Section 5.

2. Homogenization of Elastic Composites

2.1 Problem statement

As a model problem, we consider a composite rod of length l composed of a periodic array of two linearly elastic, homogeneous and isotropic constituents with perfect interfaces as illustrated in Fig.1. The rod is fixed at one end and subjected to an impact load $P(t)$ at the other end. Let the origin of the Cartesian coordinate system be located at the fixed end.

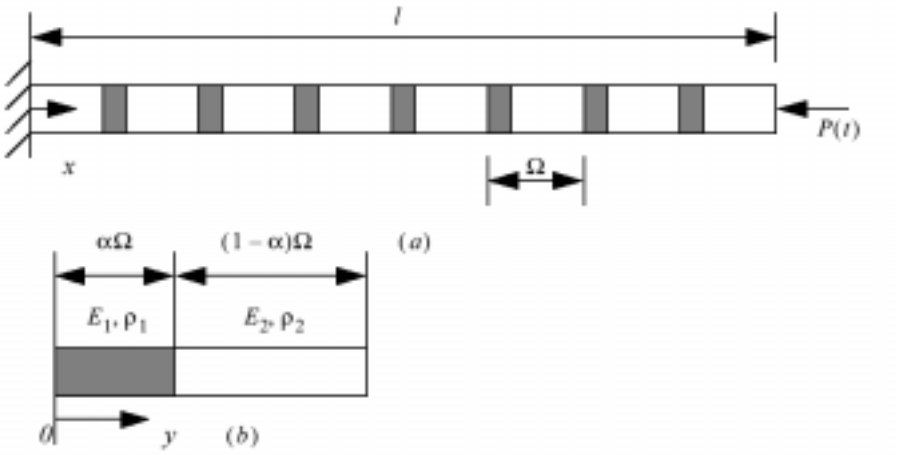

Fig.1: Composite rod subjected to an impact load: (a) Macro-problem; (b) Unit cell.

The governing elastodynamic equations are:

- Equations of motion, kinematic and constitutive equations

$$\rho(x)\ddot{u}(x,t) - (E(x)u_{,x})_{,x} = 0\,, \quad \sigma(x,t) = E(x)u_{,x} \tag{1}$$

- Interface continuity conditions

$$[u(x,t)] = 0\,, \quad [\sigma(x,t)] = 0 \tag{2}$$

- Boundary conditions

$$u(0,t) = 0\,, \quad u_{,x}(l,t) = \frac{P(t)}{E(l)A} \tag{3}$$

- Initial conditions

$$u(x, 0) = \dot{u}(x, 0) = 0 \tag{4}$$

where $u(x, t)$ and $\sigma(x, t)$ denote the axial displacement and stress, respectively; $\rho(x)$ the mass density; $E(x)$ the elastic modulus. A represents the cross-sectional area of the rod; $[\ ]$ denotes the jump operator; $(\ )_{,x}$ and the superposed dot denotes differentiation in space and time, respectively.

Conditions (1)-(4) define the initial/boundary-value problem. Since the size of heterogeneity is much smaller than the length of the bar, the direct solution of this problem is computationally infeasible. Thus the primary goal is to replace the source heterogeneous problem by a homogenized one with equivalent material properties, which could be either local or nonlocal. This is accomplished by the method of multiple-scale asymptotic expansion.

2.2 Asymptotic analysis with multiple scales

Under the premise that the composite macro reference length L is much larger than the unit cell dimension Ω, i.e. $\varepsilon = \Omega/L = (\omega\Omega)/c = k\Omega \ll 1$, where ω, k and c are the angular frequency, wave number and wave speed of the macro-wave, respectively, it is convenient to introduce a microscopic length variable y such that

$$y = x/\varepsilon \tag{5}$$

Since the response quantities u and σ depend on both x and $y = x/\varepsilon$, a two-scale asymptotic expansion is employed to approximate the displacement and stress fields

$$u(x, y, t) = \sum_{i=0}^{n} \varepsilon^i u_i(x, y, t), \qquad \sigma(x, y, t) = \sum_{i=-1}^{n} \varepsilon^i \sigma_i(x, y, t) \tag{6}$$

The periodicity of the microstructure induces the same periodicity on functions u_i and σ_i with respect to variable y. The homogenization process consists of inserting asymptotic expansions (6) into the governing equation (1), identifying the terms with equal power of ε, and finally, solving the problems obtained.

Following this process and expressing the spatial derivative in terms of $(\ )_{,x} + \varepsilon^{-1}(\ )_{,y}$, yields various order equilibrium equations

$$O(\varepsilon^{-2}): \quad (Eu_{0,y})_{,y} = 0$$

$$O(\varepsilon^{-1}): \qquad (Eu_{0,y})_{,x} + (Eu_{0,x})_{,y} + (Eu_{1,y})_{,y} = 0$$

$$O(\varepsilon^i): \rho \ddot{u}_i - \{E(u_{i,x} + u_{i+1,y})\}_{,x} - \{E(u_{i+1,x} + u_{i+2,y})\}_{,y} = 0 \quad (i = 0, 1, \ldots n) \tag{7}$$

Stresses of different orders are expressed as

$$\sigma_{-1} = E u_{0,y}$$

$$\sigma_i = E(u_{i,x} + u_{i+1,y}) \quad (i = 0, 1, \ldots n) \tag{8}$$

2.3 Macroscopic description of homogenized material

First, we consider the $O(\varepsilon^{-2})$ equilibrium equation (7). Premultiplying it by u_0, then integrating it over the unit cell domain, and finally performing integration by parts yields

$$u_0(E u_{0,y})\Big|_0^{\Omega} - \int_{\Omega} E(u_{0,y})^2 dy = 0 \tag{9}$$

The first term in (9) vanishes due to periodicity of the boundary conditions in the unit cell, which yields

$$u_{0,y} = 0 \Rightarrow u_0 = U_0(x, t) \tag{10}$$

Inserting eqn (10) into (8) leads

$$\sigma_{-1} = 0 \tag{11}$$

Next, we proceed to the $O(\varepsilon^{-1})$ equilibrium equation (7). Taking into account $u_0 = U_0(x, t)$, we have

$$\{E(U_{0,x} + u_{1,y})\}_{,y} = 0 \tag{12}$$

Due to linearity of the problem, the general solution of (12) is

$$u_1(x, y, t) = U_1(x, t) + L(y) U_{0,x} \tag{13}$$

Substituting eqn (13) into (12) and (8) for *i = 0* yields

$$\{E(1 + L_{,y})\}_{,y} = 0 \tag{14}$$

$$\sigma_0 = U_{0,x} E(1 + L_{,y}) \tag{15}$$

We now consider the unit cell given in Fig.1(b). The cell domain consists of subdomains $A^{(1)}$ and $A^{(2)}$, occupied by microconstituents 1 and 2, respectively, such that

$$A^{(1)} = [y \mid 0 < y < \alpha\Omega], \quad A^{(2)} = [y \mid \alpha\Omega < y < \Omega] \tag{16}$$

where $0 \le \alpha \le 1$ is the volume fraction of the unit cell.

Equations (14) and (15) can be written over a unit cell domain as

$$E_j(1 + L_{j,y}) = a_j\,, \quad \sigma_0^{(j)} = U_{0,x}E_j(1 + L_{j,y}) \quad (j = 1, 2) \tag{17}$$

where a_j are constants. $L_j(y)$ can be solved for from the following conditions

(a) Periodicity: $u_1(y = 0) = u_1(y = \Omega)\,, \quad \sigma_0(y = 0) = \sigma_0(y = \Omega)$

(b) Continuity: $[u_1(y = \alpha\Omega)] = 0\,, \quad [\sigma_0(y = \alpha\Omega)] = 0$

(c) Normalization: $\langle u_1(x, y, t)\rangle = U_1(x, t) \Rightarrow \langle L(y)\rangle = 0$ (18)

where

$$\langle \bullet \rangle = \frac{1}{\Omega}\sum_{j=1}^{2}\int_{A^{(j)}} \bullet \, dy \tag{19}$$

is an averaging operator. Solving for (18) yields

$$L_1(y) = \frac{(1-\alpha)(E_2 - E_1)}{(1-\alpha)E_1 + \alpha E_2}\left[y - \frac{\alpha\Omega}{2}\right],\ L_2(y) = \frac{\alpha(E_1 - E_2)}{(1-\alpha)E_1 + \alpha E_2}\left[y - \frac{(1+\alpha)\Omega}{2}\right] \tag{20}$$

$$E_n = \langle E(1 + L_{,y})\rangle = \frac{E_1E_2}{(1-\alpha)E_1 + \alpha E_2} \tag{21}$$

2.3.1 $O(\varepsilon^0)$ equilibrium

Consider the equilibrium equation of $O(\varepsilon^0)$

$$\rho\ddot{u}_0 - \{E(u_{0,x} + u_{1,y})\}_{,x} - \{E(u_{1,x} + u_{2,y})\}_{,y} = 0 \tag{22}$$

Integrating (22) over the unit cell domain and taking into account periodicity of σ_1, yields

$$\rho_n\ddot{U}_0 - E_nU_{0,xx} = 0 \tag{23}$$

where

$$\rho_n = \langle\rho\rangle = \alpha\rho_1 + (1-\alpha)\rho_2 \tag{24}$$

ρ_n and E_n are the homogenized mass density and elastic modulus of the composite. It can be seen that the homogenized material properties are the same as in statics. Thus the zero-order homogenization model is non-dispersive. In order to capture the dispersion effect, higher-order terms will be considered now.

2.3.2 $O(\varepsilon)$ equilibrium

Substituting (13) and (23) into $O(\varepsilon^0)$ equilibrium equation (22) yields

$$\{E(u_{2,y} + U_{1,x} + LU_{0,xx})\}_{,y} = E_n(\beta - 1)U_{0,xx} \tag{25}$$

where

$$\beta(y) = \frac{\rho(y)}{\rho_n} \tag{26}$$

Due to linearity of the problem, the general solution for u_2 can be expressed as

$$u_2(x, y, t) = U_2(x, t) + L(y)U_{1,x} + P(y)U_{0,xx} \tag{27}$$

Substituting (27) into (25) and (8) for $i = 1$ yields

$$\{E(L + P_{,y})\}_{,y} = E_n(\beta - 1) \tag{28}$$

$$\sigma_1 = E(1 + L_{,y})U_{1,x} + E(L + P_{,y})U_{0,xx} \tag{29}$$

From periodicity and continuity of u_2, σ_1, and normalization of u_2, i.e.

$$\langle u_2(x, y, t)\rangle = U_2(x, t) \Rightarrow \langle P(y)\rangle = 0 \tag{30}$$

follows the solution of $P(y)$. After $P(y)$ is determined, we calculate

$$\langle \rho L\rangle = 0, \quad \langle E(L + P_{,y})\rangle = 0, \quad \langle E(u_{1,x} + u_{2,y})\rangle = E_n U_{1,x} \tag{31}$$

and obtain the $O(\varepsilon)$ equilibrium equation

$$\rho\ddot{u}_1 - \{E(u_{1,x} + u_{2,y})\}_{,x} - \{E(u_{2,x} + u_{3,y})\}_{,y} = 0 \tag{32}$$

Integrating (32) over the unit cell and taking into account periodicity of σ_2, yields

$$\langle\rho\rangle\ddot{U}_1 + \langle\rho L\rangle\ddot{U}_{0,x} - \{E(u_{1,x} + u_{2,y})\}_{,x} = 0 \tag{33}$$

Inserting (31) into (33) gives

$$\rho_n \ddot{U}_1 - E_n U_{1,xx} = 0 \tag{34}$$

2.3.3 $O(\varepsilon^2)$ equilibrium

Substituting (13), (27) and (34) into the $O(\varepsilon)$ equilibrium equation (32), yields

$$\{E(u_{3,y} + PU_{0,xxx} + LU_{1,xx} + U_{2,x})\}_{,y} = E_n(\beta - 1)U_{1,xx} +$$

$$\{E_n \beta L - E(L + P_{,y})\}U_{0,xxx} \tag{35}$$

Due to linearity of (35) the general solution for u_3 is given as

$$u_3(x, y, t) = U_3(x, t) + L(y)U_{2,x} + P(y)U_{1,xx} + Q(y)U_{0,xxx} \tag{36}$$

Substituting (36) into (35) and (8) for $i = 2$ gives

$$\{E(P + Q_{,y})\}_{,y} = E_n \beta L - E(L + P_{,y}) \tag{37}$$

$$\sigma_2 = E_n U_{2,x} + E(L + P_{,y})U_{1,xx} + E(P + Q_{,y})U_{0,xxx} \tag{38}$$

where $Q(y)$ can be determined from the periodicity and continuity conditions on u_3 and σ_2 over the unit cell domain as well as the normalization condition $\langle Q(y) \rangle = 0$. After $Q(y)$ has been determined, we can calculate $\langle \rho P \rangle$ and $\langle E(P + Q_{,y}) \rangle$.

Consider the $O(\varepsilon^2)$ equilibrium equation:

$$\rho \ddot{u}_2 - \{E(u_{2,x} + u_{3,y})\}_{,x} - \{E(u_{3,x} + u_{4,y})\}_{,y} = 0 \tag{39}$$

Integrating (39) over the unit cell and taking into account periodicity of σ_3 yields

$$\rho_n \ddot{U}_2 + \langle \rho L \rangle \ddot{U}_{1,x} + \langle \rho P \rangle \ddot{U}_{0,xx} - E_n U_{2,xx} - \langle E(L + P_{,y}) \rangle U_{1,xxx} -$$

$$\langle E(P + Q_{,y}) \rangle U_{0,xxxx} = 0 \tag{40}$$

Substituting (31) and into (40) and making use of the macroscopic equation of motion (23) for U_0 gives the second order macroscopic equation of motion

$$\rho_n \ddot{U}_2 - E_n U_{2,xx} = E_d U_{0,xxxx} \tag{41}$$

where

$$E_d = \frac{[\alpha(1-\alpha)]^2(E_1\rho_1 - E_2\rho_2)^2 E_n \Omega^2}{12\rho_n^2[(1-\alpha)E_1 + \alpha E_2]^2} \tag{42}$$

E_d characterizes the effect of heterogeneity on the macroscopic behavior. It can be seen that E_d is proportional to the square of the unit cell size and vanishes for homogeneous material ($\alpha = 0$ or $\alpha = 1$). The forcing term in (41) is also proportional to the gradients of the macroscopic strain $U_{0,xxxx}$. Thus, the smaller the gradient of the macroscopic strain is, the smaller the forcing term will be.

2.3.4 $O(\varepsilon^3)$ equilibrium

$u_4(x, y, t)$ can be solved from the $O(\varepsilon^2)$ equilibrium equation (39). Due to linearity, the general solution for u_4 is as follows

$$u_4(x, y, t) = U_4(x, t) + L(y)U_{3,x} + P(y)U_{2,xx} + Q(y)U_{1,xxx} + R(y)U_{0,xxxx} \tag{43}$$

Substituting (43), (36) and (27) for $u_4(x, y, t)$, $u_3(x, y, t)$ and $u_2(x, y, t)$, respectively, into eqns (39) and (8) for $i = 3$, and making use of the macroscopic equation of motion (41) for U_2, we arrive at

$$\{E(Q + R_{,y})\}_{,y} = \beta(E_n P - E_d) - E(P + Q_{,y}) \tag{44}$$

$$\sigma_3 = E_n U_{3,x} + E(L + P_{,y})U_{2,xx} + E(P + Q_{,y})U_{1,xxx} + E(Q + R_{,y})U_{0,xxxx} \tag{45}$$

The expression for $R(y)$ can be determined from the periodicity and continuity conditions of u_4 and σ_3 over the unit cell domain as well as the normalization condition $\langle R(y)\rangle = 0$. After $R(y)$ is determined, we calculate

$$\langle \rho Q\rangle = 0, \quad \langle E(Q + R_{,y})\rangle = 0 \tag{46}$$

and obtain the $O(\varepsilon^3)$ equilibrium equation:

$$\rho\ddot{u}_3 - \{E(u_{3,x} + u_{4,y})\}_{,x} - \{E(u_{4,x} + u_{5,y})\}_{,y} = 0 \tag{47}$$

Integrating (47) over the unit cell domain and accounting for periodicity of σ_4 yields

$$\rho_n\ddot{U}_3 + \langle \rho L\rangle\ddot{U}_{2,x} + \langle \rho P\rangle\ddot{U}_{1,xx} + \langle \rho Q\rangle\ddot{U}_{0,xxx} = E_n U_{3,xx} +$$

$$\langle E(L + P_{,y})\rangle U_{2,xxx} + \langle E(P + Q_{,y})\rangle U_{1,xxxx} + \langle E(Q + R_{,y})\rangle U_{0,xxxxx} \tag{48}$$

Substituting (31), and (46) into (48) and making use of the macroscopic equation of motion (34) for U_1, we arrive at the macroscopic equation of motion for U_3

$$\rho_n \ddot{U}_3 - E_n U_{3,xx} = E_d U_{1,xxxx} \tag{49}$$

2.3.5 $O(\varepsilon^4)$ equilibrium

$u_5(x, y, t)$ can be solved from the equilibrium equation of $O(\varepsilon^3)$ (47). Due to linearity of the problem, the general solution for u_5 is as follows

$$u_5(x, y, t) = U_5(x, t) + L(y)U_{4,x} + P(y)U_{3,xx} + Q(y)U_{2,xxx} +$$

$$R(y)U_{1,xxxx} + S(y)U_{0,xxxxx} \tag{50}$$

Substituting (50), (43) and (36) for $u_5(x, y, t)$, $u_4(x, y, t)$ and $u_3(x, y, t)$, respectively, into eqns (47) and (8) for $i = 4$, and making use of the macroscopic equation of motion (49) for U_3, yields

$$[E(R + S_{,y})]_{,y} = \beta(E_n Q - E_d L) - E(Q + R_{,y}) \tag{51}$$

$$\sigma_4 = E_n U_{4,x} + E(L + P_{,y})U_{3,xx} + E(P + Q_{,y})U_{2,xxx} +$$

$$E(Q + R_{,y})U_{1,xxxx} + E(R + S_{,y})U_{0,xxxxx} \tag{52}$$

$S(y)$ can be determined from the periodicity and continuity conditions of u_5 and σ_4 over the unit cell domain as well as the normalization condition $\langle S(y) \rangle = 0$. After $S(y)$ has been determined, we can calculate $\langle \rho R \rangle$.

The resulting $O(\varepsilon^4)$ equilibrium equation is given as

$$\rho \ddot{u}_4 - \{E(u_{4,x} + u_{5,y})\}_{,x} - \{E(u_{5,x} + u_{6,y})\}_{,y} = 0 \tag{53}$$

Integrating (53) over the unit cell and accounting for the periodicity of σ_5 yields

$$\rho_n \ddot{U}_4 + \langle \rho L \rangle \ddot{U}_{3,x} + \langle \rho P \rangle \ddot{U}_{2,xx} + \langle \rho Q \rangle \ddot{U}_{1,xxx} + \langle \rho R \rangle \ddot{U}_{0,xxxx}$$

$$= E_n U_{4,xx} + \langle E(L + P_{,y}) \rangle U_{3,xxx} + \langle E(P + Q_{,y}) \rangle U_{2,xxxx} +$$

$$\langle E(Q + R_{,y}) \rangle U_{1,xxxxx} + \langle E(R + S_{,y}) \rangle U_{0,xxxxxx} \tag{54}$$

Inserting eqns (31), , (46) into (54) and making use of the macroscopic equations of motion (23) and (41) for U_0 and U_2 respectively, we arrive at the macroscopic equation of motion for U_4

$$\rho_n \ddot{U}_4 - E_n U_{4,xx} = E_d U_{2,xxxx} - E_g U_{0,xxxxxx} \tag{55}$$

where

$$E_g = \frac{[\alpha(1-\alpha)]^2 (E_1\rho_1 - E_2\rho_2)^2 E_n \Omega^4}{360\rho_n^4[(1-\alpha)E_1 + \alpha E_2]^4}\{\alpha^2 E_2^2[2\alpha^2\rho_1^2 - (1-\alpha)^2\rho_2^2 +$$

$$6\alpha(1-\alpha)\rho_1\rho_2] + 2\alpha(1-\alpha)E_1E_2[3\alpha^2\rho_1^2 + 3(1-\alpha)^2\rho_2^2 + 11\alpha(1-\alpha)\rho_1\rho_2] -$$

$$(1-\alpha)^2 E_1^2[\alpha^2\rho_1^2 - 2(1-\alpha)^2\rho_2^2 - 6\alpha(1-\alpha)\rho_1\rho_2]\} \tag{56}$$

E_g characterizes the effect of the microstructure on the macroscopic behavior. It has a strong dependency on the unit cell size (fourth power of Ω). Note that for a homogeneous material, E_g and E_d vanish. The forcing term in the fourth order macroscopic equation of motion appears to be in the form of E_d multiplied by the gradients of the second-order macroscopic strain, $U_{2,xxxx}$, and the product of E_g and the gradients of the zero-order macroscopic strain, $U_{0,xxxxxx}$. The initial and boundary conditions for the model problem are given as follows:

$$\text{ICs:} \quad U_i(x,0) = \dot{U}_i(x,0) = 0 \qquad (i = 0, 1, 2, 3, 4) \tag{57}$$

$$\text{BCs:} \quad U_0(0,t) = 0, \; U_{0,x}(l,t) = \frac{P(t)}{E_n A}$$

$$U_i(0,t) = 0, \quad U_{i,x}(l,t) = 0 \qquad (i = 1, 2, 3, 4) \tag{58}$$

From the above equations of motion and boundary conditions, we can observe that

$$U_3 = U_1 \equiv 0 \tag{59}$$

It has been shown in [17] that the first and the third order terms introduce the effects of polarization and attenuation, respectively. These terms vanish for macroscopically isotropic materials. Moreover, if the size of the microstructure, Ω, is infinitesimal, E_d and E_g in (42) and (56) vanish, and the higher order corrections, U_2 and U_4, disappear. Thus if the size of heterogeneity is very small, the dispersion effect is negligible. Moreover, if the impedances, ($Z = \sqrt{E\rho}$), of the two microconstituents are identical, i.e., $E_1\rho_1 = E_2\rho_2$,

E_d and E_g will also vanish. From the physical point of view, this means that there is no reflections at the material interfaces, making the waves non-dispersive.

3. Solution of Macroscopic Equations

3.1 The analytical solution

The simplicity of the macroscopic equations of motion and corresponding boundary conditions in 1-D permits for closed-form representation of the solutions. In the following we will obtain such a closed-form solution using Laplace transform.

First, we begin with the zero-order equation of motion (23). Taking the Laplace transform of (23) with respect to time yields

$$s^2\bar{U}_0(x,s) - sU_0(x,0) - \dot{U}_0(x,0) - c^2(\bar{U}_0(x,s))_{,xx} = 0 \tag{60}$$

where

$$c = \sqrt{E_n/\rho_n} \tag{61}$$

is the homogenized wave speed and $\bar{U}_0(x,s)$ is the Laplace transform of $U_0(x,t)$. Inserting the initial conditions (57) into (60) yields

$$s^2\bar{U}_0(x,s) - c^2(\bar{U}_0(x,s))_{,xx} = 0 \tag{62}$$

The general solution of (62) is

$$\bar{U}_0(x,s) = B_1\cosh\frac{sx}{c} + B_2\sinh\frac{sx}{c} \tag{63}$$

where B_1 and B_2 are constants. Taking Laplace transform of the boundary conditions (58) for U_0 gives

$$U_0(0,s) = 0, \quad \bar{U}_{0,x}(l,s) = \frac{L[P(t)]}{E_nA} \tag{64}$$

Inserting (63) into (64) yields

$$B_1 = 0, \quad B_2 = \frac{c}{E_nA}\frac{L[P(t)]}{s\cosh\frac{sl}{c}} \tag{65}$$

Thus, the solution of $\bar{U}_0(x,s)$ becomes

$$\bar{U}_0(x,s) = \frac{c}{E_n A}\frac{\sinh\frac{sx}{c}}{s\cosh\frac{sl}{c}}L[P(t)] \tag{66}$$

We consider the impact load in the form

$$P(t) = P_0 f(t) \tag{67}$$

where P_0 is a constant which specifies the magnitude of the impact load and $0 \le f(t) \le 1$ is a time function which specifies variation of the impact load with time. We consider the following time dependent function

$$f(t) = a_0 t^4 (t-T)^4 [1 - H(t-T)] \tag{68}$$

where $H(t)$ is the Heaviside function, T the duration of the pulse; a_0 is a scaling coefficient, which makes $0 \le f(t) \le 1$, given by

$$a_0 = 1/max[t^4(t-T)^4(1-H(t-T))] = 16^2/T^8 \tag{69}$$

Taking the Laplace transform of $f(t)$ and substituting it into (66) yields

$$\bar{U}_0(x,s) = \frac{P_0 a_0 c}{E_n A}\frac{\sinh\frac{sx}{c}}{s\cosh\frac{sl}{c}}\left[\left(\frac{8!}{s^9} + \frac{6\times 6! T^2}{s^7} + \frac{4! T^4}{s^5}\right)(1-e^{-sT}) - \right.$$

$$\left. 4T\left(\frac{7!}{s^8} + \frac{5! T^2}{s^6}\right)(1+e^{-sT})\right] \tag{70}$$

$U_0(x,t)$ is found by taking the inverse Laplace transform of $\bar{U}_0(x,s)$ as

$$U_0(x,t) = L^{-1}[\bar{U}_0(x,s)] = \frac{2048 P_0 l}{\pi^2 E_n A}\sum_{m=1}^{\infty}\frac{\sin(\bar{p}\bar{x})G_0(m,\dot{t},\bar{d},\bar{D})}{(-1)^{m-1}(2m-1)^2} \tag{71}$$

where

$$\dot{t} = t/T, \quad \bar{x} = x/l, \quad \bar{p} = (2m-1)\pi/2, \quad \bar{d} = ct/l, \quad D = cT/l \tag{72}$$

and G_0 is a the non-dimensionalized time function, which can be found in the closed form.

Now that we have obtained the analytical solution of $U_0(x, t)$, we proceed to solve for the second order equation of motion (41). Taking the fourth derivative of $U_0(x, t)$ with respect to x and substituting the result into (41) yields

$$U_2(x, t) = \frac{16384 P_0 l^3 \Omega^2}{\pi^4 E_n A (cT)^4} \frac{[\alpha(1-\alpha)(E_1\rho_1 - E_2\rho_2)]^2}{\rho_n^2[(1-\alpha)E_1 + \alpha E_2]^2} \sum_{m=1}^{\infty} \frac{\sin(\bar{p}\bar{x}) G_2(m, \dot{t}, \bar{d}, \bar{D})}{(-1)^{m-1}(2m-1)^4} \tag{73}$$

where G_2 is another non-dimensionalized time function, which can be found in the closed form.

For $t > T$, the value of the Heaviside function $H(\dot{t} - 1)$ becomes unity and it can be shown that the non-secular terms in $U_2(x, t)$ are negligible compared with secular terms. Under this condition, G_0 and G_2 can be simplified as

$$G_0(m, \dot{t}, \bar{d}, \bar{D}) = (24/\bar{D}^4)\bar{G}_0(m, \dot{t}, \bar{d}, \bar{D}) \tag{74}$$

$$G_2(m, \dot{t}, \bar{d}, \bar{D}) = \dot{t}\bar{G}_2(m, \dot{t}, \bar{d}, \bar{D}) \tag{75}$$

where

$$\bar{G}_0(m, \dot{t}, \bar{d}, \bar{D}) = -\frac{1}{\bar{p}^4}\left\{\frac{20}{\bar{p}\bar{D}}\left[\frac{42}{(\bar{p}\bar{D})^2} - 1\right][\sin(\bar{p}\bar{d}) + \sin(\bar{p}(\bar{d} - \bar{D}))] + \right.$$

$$\left.\left[\frac{1680}{(\bar{p}\bar{D})^4} - \frac{180}{(\bar{p}\bar{D})^2} + 1\right][\cos(\bar{p}\bar{d}) - \cos(\bar{p}(\bar{d} - \bar{D}))]\right\} \tag{76}$$

$$\bar{G}_2(m, \dot{t}, \bar{d}, \bar{D}) = 10\left[\frac{42}{(\bar{p}\bar{D})^2} - 1\right][\cos(\bar{p}\bar{d}) + \cos(\bar{p}(\bar{d} - \bar{D}))] -$$

$$\frac{\bar{p}\bar{D}}{2}\left[\frac{1680}{(\bar{p}\bar{D})^4} - \frac{180}{(\bar{p}\bar{D})^2} + 1\right][\sin(\bar{p}\bar{d}) - \sin(\bar{p}(\bar{d} - \bar{D}))] \tag{77}$$

The expression for G_2 indicates that the peak values of $U_2(x, t)$ grow linearly with time, and when time approaches infinity, $U_2(x, t)$ becomes unbounded.

After the solutions of $U_0(x, t)$ and $U_2(x, t)$ have been obtained, we solve for $U_4(x, t)$ following the same procedures. Owing to the limited space, the analytical solution is not presented here.

Based on the analytical solutions for $U_0(x, t)$ and $U_2(x, t)$, we can estimate the value of ε for the case of $t > T$:

$$\varepsilon = \sqrt{\frac{\left\|\varepsilon^2 U_2\right\|_{0,\Omega}}{\left\|U_0\right\|_{0,\Omega}}}$$

$$= \frac{\sqrt{3}\alpha(1-\alpha)\left|E_1\rho_1 - E_2\rho_2\right|}{3\pi\rho_n[(1-\alpha)E_1 + \alpha E_2]}\frac{\Omega}{l}\sqrt{\frac{t}{T}}\; f(cT/l, \sin(\omega_1 ct/l), \cos(\omega_2 ct/l)) \tag{78}$$

where ω_1 and ω_2 are constants and $\|\cdot\|_{0,\Omega}$ is a L_2 norm defined as

$$\|g(x)\|_{0,\Omega} = \left[\int_{(x_0-\Omega/2)}^{(x_0+\Omega/2)} |g(x)|^2\right]^{1/2} \tag{79}$$

with x_0 being the center of the unit cell, and

$$f(cT/l, \sin(\omega_1 ct/l), \cos(\omega_2 ct/l)) = \sqrt{\frac{\left\|g_2\right\|_{0,\Omega}}{\left\|g_0\right\|_{0,\Omega}}} \tag{80}$$

$$g_2 = \sum_{m=1}^{\infty} \frac{\sin(\bar{p}\bar{x})\bar{G}_2(m, \dot{t}, \bar{d}, \bar{D})}{(-1)^{m-1}(2m-1)^4}, \quad g_0 = \sum_{m=1}^{\infty} \frac{\sin(\bar{p}\bar{x})\bar{G}_0(m, \dot{t}, \bar{d}, \bar{D})}{(-1)^{m-1}(2m-1)^2} \tag{81}$$

It can be observed that the value of ε depends on four factors: (i) the normalized square of the impedance mismatch, (ii) the normalized unit cell size Ω/l, (iii) the normalized square root of time, and (iv) the pulse duration T. It can be numerically shown that the function $f(cT/l, \sin(\omega_1 ct/l), \cos(\omega_2 ct/l))$ rapidly increases with decrease in pulse duration T.

The value of scaling parameter, ε, is an important indicator of the validity of the asymptotic expansion. The asymptotic sequence is considered to be uniformly valid for small values of ε.

3.2 The finite element solution

In this section, we establish numerical procedures for solving the macroscopic equations of motion. These procedures are directly applicable for multidimensional case.

The zero-order equation of motion can be solved by the finite element method. Here we focus on the solution of the second order equation of motion (41) requiring recovery of higher order derivatives.

The weak form of the second order equation of motion (41) is given by

$$\int_0^l w\rho_n A\ddot{U}_2 dx - \int_0^l wE_n AU_{2,xx} dx = \int_0^l wE_d AU_{0,xxxx} dx \qquad \forall w \in C^0 \tag{82}$$

where w is a weighting function. Integrating the above equation by parts yields

$$\int_0^l w\rho_n A\ddot{U}_2 dx + \int_0^l E_n Aw_{,x} U_{2,x} dx = -\int_0^l E_d Aw_{,x} U_{0,xxx} dx +$$

$$[wE_d AU_{0,xxx} + wE_n AU_{2,x}]\Big|_0^l \qquad \forall w \in C^0 \tag{83}$$

Given the natural boundary condition, $U_{2,x}(l,t) = 0$, and the fact that $w(x=0) = 0$ where the essential boundary conditions are prescribed, the above equation reduces to

$$\int_0^l w\rho_n A\ddot{U}_2 dx + \int_0^l E_n Aw_{,x} U_{2,x} dx = -\int_0^l E_d Aw_{,x} U_{0,xxx} dx + [wE_d AU_{0,xxx}]\Big|_{x=l} \tag{84}$$

The solution and weighting functions are interpolated as

$$U_0^e = \boldsymbol{N}\boldsymbol{d}_{\boldsymbol{0}}^{\boldsymbol{e}}, \qquad U_2^e = \boldsymbol{N}\boldsymbol{d}_{\boldsymbol{2}}^{\boldsymbol{e}}, \qquad w = \boldsymbol{N}\phi \tag{85}$$

where $\boldsymbol{N}$ are the shape functions. Substituting eqn (85) into (84) yields

$$\int_0^l \rho_n A\boldsymbol{N}^{\boldsymbol{T}}\boldsymbol{N}\ddot{\boldsymbol{d}}_{\boldsymbol{2}}^{\boldsymbol{e}} dx + \int_0^l E_n A\boldsymbol{B}^{\boldsymbol{T}}\boldsymbol{B}\boldsymbol{d}_{\boldsymbol{2}}^{\boldsymbol{e}} dx = -\int_0^l E_d A\boldsymbol{B}^{\boldsymbol{T}}\boldsymbol{N}\boldsymbol{d}_{\boldsymbol{0,xxx}}^{\boldsymbol{e}} dx + [E_d A\boldsymbol{N}^{\boldsymbol{T}}\boldsymbol{d}_{\boldsymbol{0,xxx}}]\Big|_{x=l} \tag{86}$$

where $\boldsymbol{B}$ denotes the derivative of the shape functions. The above equation can be written in the matrix form

$$\boldsymbol{M}\ddot{\boldsymbol{d}}_{\boldsymbol{2}} + \boldsymbol{K}\boldsymbol{d}_{\boldsymbol{2}} = \boldsymbol{F}(t) \tag{87}$$

where

$$\boldsymbol{M} = \sum_{e=1}^{Ne} \boldsymbol{m}^{\boldsymbol{e}}, \quad \boldsymbol{K} = \sum_{e=1}^{Ne} \boldsymbol{k}^{\boldsymbol{e}}$$

$$\boldsymbol{F}(t) = -\sum_{e=1}^{Ne} \boldsymbol{h^e d^e_{0,xxx}} + [E_d A \boldsymbol{d_{0,xxx}}]\Big|_{x=l} \tag{88}$$

$\boldsymbol{M}, \boldsymbol{K}$ and $\boldsymbol{F}(t)$ are the overall mass matrix, stiffness matrix and load vector, respectively. *Ne* denotes the number of elements in the mesh. The element matrices are

$$\boldsymbol{m^e} = \int_{l_e} \rho_n A \boldsymbol{N^T N} dx, \quad \boldsymbol{k^e} = \int_{l_e} E_n A \boldsymbol{B^T B} dx, \quad \boldsymbol{h^e} = \int_{l_e} E_d A \boldsymbol{B^T N} dx \tag{89}$$

where l_e is the length of the element.

The challenge is to accurately recover higher order derivatives, such as $\boldsymbol{d_{0,xxx}}$. Here, we employ Wiberg's modification [21] of the superconvergent patch recovery (SPR) technique originally developed by Zienkiewicz and Zhu [20]. Wiberg et. al. [21] proposed the superconvergent patch recovery technique incorporating equilibrium equations in a patch as well as boundary conditions at boundary points (SPREB), for patches near boundaries where tractions and displacements are prescribed. The method involves a weighted least-squares polynomial fit in an attempt to force the recovered solution to satisfy the appropriate boundary conditions.

The direct finite element solution of derivatives

$$U^h_{0,x} = \boldsymbol{B d^e_0}, \quad \sigma^h_0 = E_n \boldsymbol{B d^e_0} \tag{90}$$

is of lower accuracy than the solution and exhibits interelement discontinuity. The superconvergent derivatives $(U^*_{0,x})$, (σ^*_0), are obtained by interpolation over a patch of elements as

$$U^*_{0,x} = \boldsymbol{X a}, \quad \sigma^*_0 = E_n U^*_{0,x} \tag{91}$$

where $\boldsymbol{a}$ is a set of unknown parameters and the monomial term in the row matrix $\boldsymbol{X}$ are those present in the shape function $\boldsymbol{N}$.

We define the following weighted residuals for the improved solution

$$R_\sigma = [w_s(\sigma^*_0 - \sigma^h_0)]_s, \quad R_{\sigma_b} = [w_b(\sigma^*_0 - \sigma^b_0)]_{\sigma_b} \tag{92}$$

where R_σ is the residual for stresses at superconvergent points (*sp*); R_{σ_b} the residual for stresses at the natural boundary (σ_b) where tractions are prescribed; w_s and w_b are the weighting coefficients.

In order to determine the unknown parameters $\boldsymbol{a}$, we define the following functional

$$\Pi(\boldsymbol{a}) = \sum_{is=1}^{ns} R_{\sigma}^2 + \sum_{ib=1}^{nb} R_{\sigma_b}^2 \tag{93}$$

where *ns* is the number of sampling points (superconvergent points) in a patch and *nb* the number of boundary points in a patch where the natural boundary conditions are prescribed. The parameters $\boldsymbol{a}$ are obtained from the minimization of the functional over local patches of elements

$$\frac{\partial \Pi}{\partial \boldsymbol{a}} = 0 \tag{94}$$

which leads to

$$\boldsymbol{C}\boldsymbol{a} = \boldsymbol{r} \tag{95}$$

where

$$\boldsymbol{C} = \sum_{is=1}^{ns} (w_s^2 E_n \boldsymbol{X}^{\boldsymbol{T}} \boldsymbol{X})_{is} + \sum_{ib=1}^{nb} (w_b^2 E_n \boldsymbol{X}^{\boldsymbol{T}} \boldsymbol{X})_{ib}$$

$$\boldsymbol{r} = \sum_{is=1}^{ns} (w_s^2 E_n \boldsymbol{X}^{\boldsymbol{T}} U_{0,x}^h)_{is} + \sum_{ib=1}^{nb} (w_b^2 \boldsymbol{X}^{\boldsymbol{T}} \sigma_0^b)_{ib} \tag{96}$$

Without loss of generality, we can set $w_s = 1$ and scale w_b accordingly. Once the parameters $\boldsymbol{a}$ are determined, the recovered nodal values of $U_{0,x}$ are calculated by insertion of appropriate coordinates into the expression for $U^*_{0,x}$. After the nodal values $\boldsymbol{d}_{\boldsymbol{0,x}}$ are recovered, we obtain

$$U_{0,x}^e = \boldsymbol{N}\boldsymbol{d}_{\boldsymbol{0,x}}^{\boldsymbol{e}}, \qquad U_{0,xx}^e = \boldsymbol{B}\boldsymbol{d}_{\boldsymbol{0,x}}^{\boldsymbol{e}} \tag{97}$$

The nodal values $\boldsymbol{d}_{\boldsymbol{0,xx}}$ can be recovered based on the known values of $\boldsymbol{d}_{\boldsymbol{0,x}}$ by following the same procedures as for the recovery of $\boldsymbol{d}_{\boldsymbol{0,x}}$ from $\boldsymbol{d}_{\boldsymbol{0}}$. $\boldsymbol{d}_{\boldsymbol{0,xxx}}$ can be recovered in a similar fashion. For recovering the derivatives higher than the first order and for patches not containing any boundary points where the natural boundary conditions are prescribed, we set $w_b = 0$.

4. Numerical example

Numerical experimentation agenda includes two test problems, both dealing with the impact of the composite rod shown in Fig.1. The first example is used to demonstrate the

influence of secular terms. The geometric parameters of the rod are as follows: length $l = 1$ *m*, cross-sectional area $A = 10^{-4}\ m^2$, unit cell size $\Omega = 0.02\ m$. The rod is subjected to an impact load $P(t) = P_0 a_0 t^4 (t-T)^4 [1 - H(t-T)]$, where $P_0 = -50\ KN$ and a_0 is scaled so that $0 \le P(t) \le P_0$. The material properties of the rod are as follows: Elastic moduli $E_1 = 120\ GPa$, $E_2 = 6\ GPa$, mass density $\rho_1 = 7000\ Kg/m^3$, $\rho_2 = 6000\ Kg/m^3$, volume fraction $\alpha = 0.5$. The homogenized material properties are calculated and are given as: $E_n = 11.43\ GPa$ and $\rho_n = 6500\ Kg/m^3$. In this case, $E_1/E_2 = 20$.

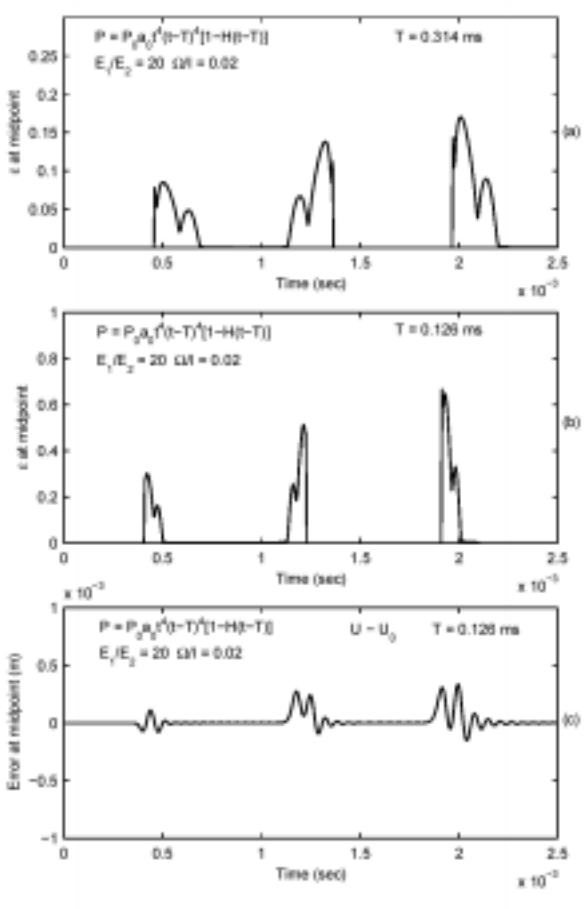

Fig.2: Quality of zero-order homogenization: (a) Estimated values of ε for $(T = 0.314ms)$; (b) Estimated values of ε for $(T = 0.126ms)$; (c) The error of the zero-order homogenization

The values of the estimated scaling parameter, ε, at the midpoint of the rod are plotted in Fig.2 (a) and (b) for pulse durations of $T = 0.314\ ms$ and $T = 0.126\ ms$, respectively. The results confirm our earlier findings indicating growth of ε with time. It can be seen that after a few reflections of the wave from macro-boundaries, the value of ε increases rendering the asymptotic sequence to be invalid. Thus the higher-order homogenization becomes not valid for very long time spans. We now focus on the time spans for which the theory is valid.

The error in the zero-order homogenization (as compared to the response of the source heterogeneous bar) for pulse duration of $T = 0.126$ is plotted in Fig. 2 (c). It can be observed that the error increases with time similarly to the growth of ε.

The second numerical example is devised to demonstrate the effectiveness of the higher-order homogenization theory in capturing the dispersion effect caused by the material heterogeneity. The geometric parameters of the rod remain the same as in the first example. The material properties in this example are: $E_1 = 200\ GPa$, $E_2 = 5\ GPa$, $\rho_1 = \rho_2 = 8000\ Kg/m^3$, and $\alpha = 0.5$. The homogenized material properties are calculated and are given as $E_n = 9.76\ GPa$ and $\rho_n = 8000\ Kg/m^3$. In this case, $E_1/E_2 = 40$. The impact load in

this example is $P(t) = P_0 b_0 t^6 (t-T)^6 [1 - H(t-T)]$, where $P_0 = -50$ *KN* and b_0 is scaled so that $0 \le P(t) \le P_0$.

First, we consider the pulse duration of $T = 0.262$ *ms*. For the reference solution of the source heterogeneous problem a very fine mesh is used. Figure 3 (a) and (b) show the plots of the reference solution at the midpoint of the rod for the source problem and the zero-order homogenization theory, respectively. The response of the source problem is averaged over the unit cell at the midpoint of the rod. For this low frequency case, the contribution of the higher-order terms is insignificant compared with the zero-order term, and the zero-order homogenization alone provides satisfactory results.

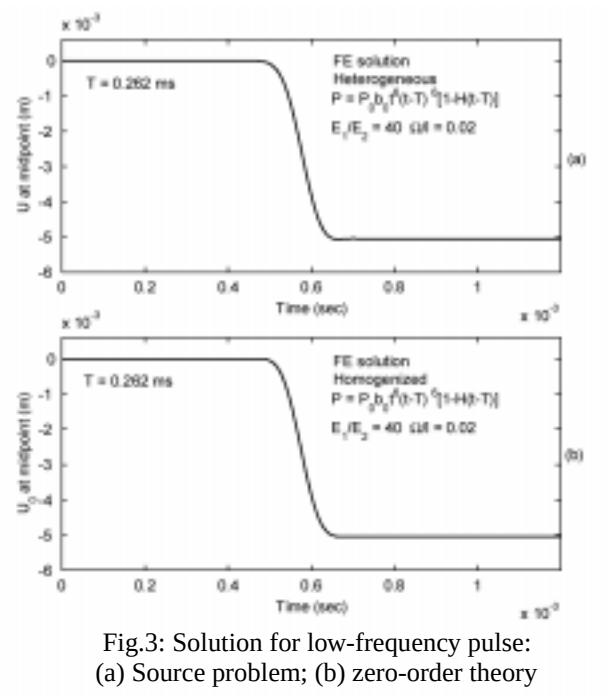

Fig.3: Solution for low-frequency pulse:
(a) Source problem; (b) zero-order theory

Next, we consider a shorter pulse duration of $T = 0.157$ ms. Finite element solution at the midpoint of the rod for the source problem and the zero-order homogenization is plotted in Fig.4 (a) and (b), respectively. The error of the zero-order homogenization, $U - U_0$, is plotted in Fig.4 (c). Figure 5 shows the corresponding responses of the higher-order homogenization as well as the higher-order correction. It can be observed that for the higher-frequency pulse, the zero-order homogenization alone is inadequate and the higher-order terms introduce the necessary correction to the zero-order method.

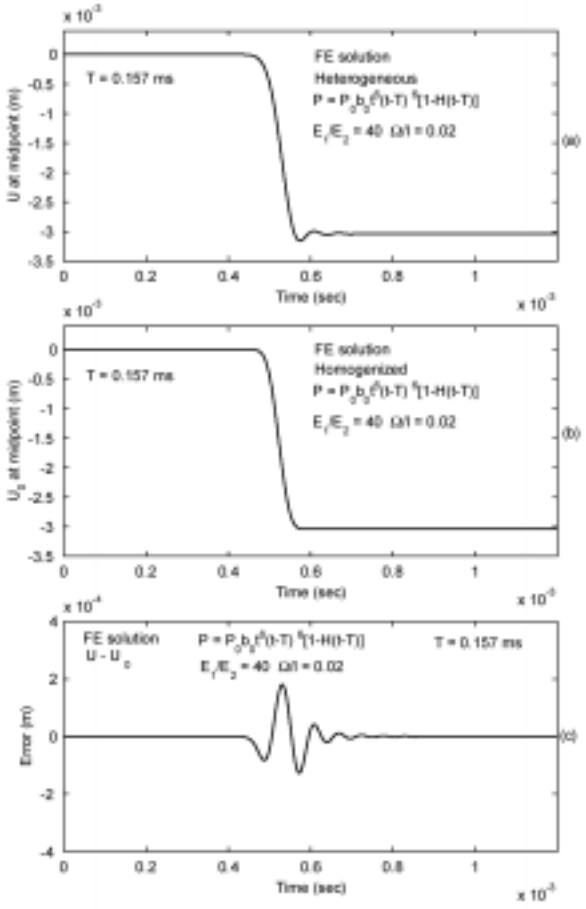

Fig.4: Quality of zero-order theory: (a) The source problem; (b) Zero-order theory; (c) The error in zero-order theory

Finally, we investigate the applicability of the FEM method for solving the higher-order homogenized equations of motion. Fig. 6 compares the analytical and finite element solutions for the second order correction, $U_2(x,t)$. In Fig.6 (a), the numerical procedure is based on recovering nodal values of the higher-order derivatives by averaging finite element solution obtained from adjacent elements. This simplistic scheme fails to accurately predict higher order derivatives as evidenced by large discrepancy compared to the analytical solution. In Fig.6 (b) the numerical procedure is based on superconvergent patch recovery technique incorporating boundary conditions (SPRB). Excellent agreement with the analytical solution has been observed.

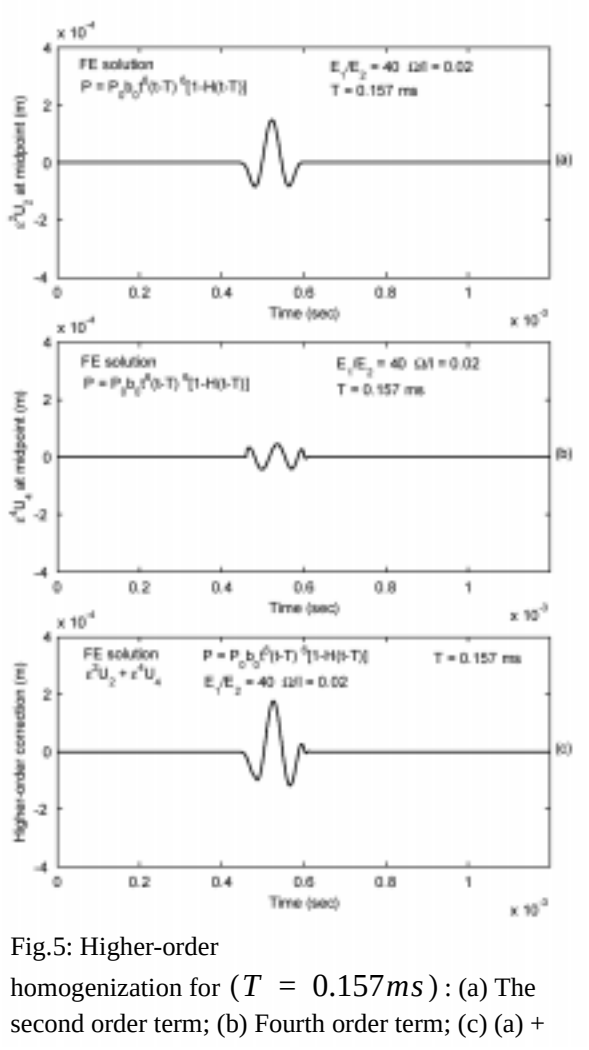

Fig.5: Higher-order homogenization for $(T = 0.157ms)$: (a) The second order term; (b) Fourth order term; (c) (a) +

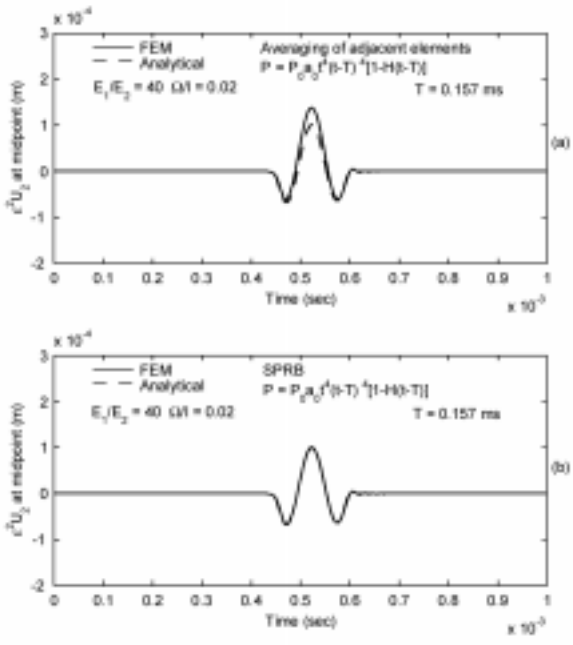

Fig.6: The analytical and finite element solutions: (a) Direct FEM recovery of derivatives; (b) FEM based on the recovery by SPRB.

5. Concluding Remarks

Fourth order homogenization theory applied to initial/boundary-value problem with oscillatory coefficients in one-dimension has been studied. It has been shown that the zero-order homogenization theory leads to non-dispersive model, while higher order theory captures dispersion effects. Validity range and limitations of the higher order theory have been established. Four factors have been identified to control the validity of the higher order theory: (i) the square of the normalized impedance mismatch, (ii) the normalized unit cell size Ω/l, (iii) the normalized square root of time, and (iv) the pulse duration T.

Future work will focus on the following four issues: (i) the influence of microstructure randomness on the dispersion effect, (ii) investigation of asymptotic expansions in space and time in attempt to extend the validity range of the current theory, (iii) adaptive construction of the multiscale computational model, and (iv) extension of the theory to multi-dimensions.

The adaptive multiscale model construction can be controlled by the estimated value of ε. At very low values of ε, $\varepsilon(\boldsymbol{x}) \le (10^{-2} \Leftrightarrow 10^{-1})$, the classical zero-order homogenization

theory is adequate, while in the intermediate range defined by $(10^{-2} \Leftrightarrow 10^{-1}) \leq \varepsilon(\boldsymbol{x}) \leq (10^{-1} \Leftrightarrow 1)$, higher order (nonlocal) terms must be employed. Finally, in the regions where $\varepsilon(\boldsymbol{x}) \geq (10^{-1} \Leftrightarrow 1)$, the model construction on the basis of the multiple scale expansion method is no longer valid, and thus the macro-scale model should contain the microscale features.

References

1 A. Bedford, D.S. Drumheller and H.J. Sutherland, On modeling the dynamics of composite materials, in: Mechanics Today, vol. 3, S. Nemat-Nasser, ed., Pergamon Press, New York, 1976.

2 J. Fish and V. Belsky, Multi-grid method for periodic heterogeneous media, Part 2: Multiscale modeling and quality control in multidimensional case, Comput. Methods Appl. Mech. Engrg. 126:17-38, 1995.

3 F.C. Moon, Wave surfaces due to impact on anisotropic plates, J. Composite Materials, 8:62-79, 1972.

4 H. Murakami and G.A. Hegemier, A mixture model for unidirectionally fiber-reinforced composites, J. Appl. Mech. 53:765-773, 1986.

5 C.T. Sun, J.D. Achenbach and G. Herrmann, Continuum theory for a laminated media, J. Appl. Mech. 35:467-475, 1968.

6 J.D. Achenbach and G. Herrmann, Dispersion of free harmonic waves in fiber-reinforced composites, AIAA J. 6:1832-1836, 1968.

7 A. Bedford and M. Stern, Toward a diffusing continuum theory of composite materials, J. Appl. Mech. 38:8-14, 1971.

8 A. Bedford and M. Stern, A multi-continuum theory for composite elastic materials, Acta Mechanica, 14: 85-102, 1972.

9 G.A. Hegemier, G.A. Gurtman and A.H. Nayfeh, A continuum mixture theory of wave propagation in laminated and fiber reinforced composites, Int. J. Solids Struct. 9:395-414, 1973.

10 G.A. Hegemier, On a theory of interacting continua for wave propagation in composites, in: Dynamics of Composite Materials, The American Society of Mechanical Engineers, E.H. Lee ed., New York, 1972.

11 T.C.T. Ting, Dynamic Response of Composites, Appl. Mech. Rev. 33:1629-1635, 1980.

12 A. Benssousan, J.L. Lions and G. Papanicoulau, Asymptotic Analysis for Periodic Structures, North Holland, Amsterdam, 1978.

13 N.S. Bakhvalov and G.P. Panasenko, Homogenization: Averaging Processes in Periodic Media, Kluwer, Dordrecht, 1989.

14 E. Sanchez-Palencia, Non-homogeneous Media and Vibration Theory, Springer, Ber-

lin, 1980.

15 B. Gambin and E. Kroner, “High order terms in the homogenized stress-strain relation of periodic elastic media,” Phys. Stat. Sol., 51: 513-519, 1989.

16 C. Boutin, Microstructural effects in elastic composites, Int. J. Solids Struct. 33(7):1023-1051, 1996.

17 C. Boutin and J.L. Auriault, Rayleigh scattering in elastic composite materials, Int. J. Engng. Sci. 31(12):1669-1689, 1993.

18 C. Boutin and J.L. Auriault, Dynamic behavior of porous media saturated by a viscoelastic fluid. Application to bituminous concretes, Int. J. Engng. Sci., 28(11):1157-1181, 1990.

19 W.T. Thomson, Laplace Transformation, Prentice-Hall, New York, 1950.

20 O.C. Zienkiewicz and J.Z. Zhu, The superconvergent patch recovery and *a posteriori* error estimates. Part 1: The recovery technique, Int. J. Numer. Methods Eng. 33:1331-1346, 1992.

21 N.E. Wiberg, F. Abdulwahab and S. Ziukas, Enhanced superconvergent patch recovery incorporating equilibrium and boundary conditions, Int. J. Numer. Methods Eng. 37:3417-3440, 1994.